EGTRIB Journal
JOURNAL OF
THE EGYPTIAN SOCIETY OF TRIBOLOGY
VOLUME 12, NO. 1, January 2015, pp. 49 - 61 **ISSN 2090 - 5882**

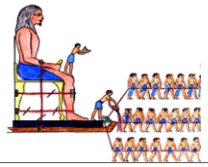

CONTACT STRESS DISTRIBUTION OF DEEP GROOVE BALL BEARING USING ABAQUS

Nabhan A.[1], Nouby M.[2], Samy A. M.[1], Mousa, M. O.[1]

[1]Faculty of Engineering, Minia University, 61111 Minia, Egypt,
[2]Faculty of Engineering, South Valley University, 83521 Qena, Egypt.

ABSTRACT

This paper examines the contact stress distribution of deep groove ball bearings through analytical and numerical methods. The contact pressure distribution between the ball and the raceway of the bearing 6004 is performed by finite element software ABAQUS. To validate the finite element model, an analytical method using Hertzian contact theory is derived by MATLAB software. Influence of shaft misalignment with different angles namely; 0.2^0, 0.4^0, 0.6^0, 0.8^0 and 1^0 is investigated. It is found that finite element analysis can be evaluated the contact stress at any point around the contact surface. It is also concluded that the shaft misalignment lead to decrease the maximum contact stress and increase the contact area between the ball and the raceway of the bearing.

KEYWORDS

Contact Stress, Hertzian Stress, Misalignment, Deep Groove Ball Bearings, Finite Element Analysis, ABAQUS.

INTRODUCTION

In most bearing applications, radial, axial, or combinations of radial and axial forces are considered. Under heavy loading; especially by hollow shafts, shaft bend can be excited. Moreover, rigidity of bearing housing has a significant effect on the machine stability especially under the action of external loads resulting from the bearing, [1]. These loading conditions tend to significant changes in bearing deflections, and hence the resulting contact stresses. The transition of the acting loads through the main parts of the anti-friction bearing; i.e. rolling elements, inner and outer races; results in a small real area of contact between rolling element and bearing races. Therefore, the elemental loads will be moderate and high stress vales will be produced.

The general method for determining the distribution of stresses in the zone of contact of two elastic bodies was indicated, [2]. The Hertzian contact stress usually refers to the stress close to the area of contact between two bodies of different radii of most interest are the basic types of contact between two bodies. The first type is bodies initially having point contact before the deformation, such as two spheres, a sphere and a plane, or a

sphere and a cylinder. The other one is bodies having straight line contact before deformation, such as two cylinders with parallel axes or a cylinder and a plane. Practical illustrations of the first type of contact are ball bearings and their supports and wheels rolling on convex rails; illustrations of the second type are roller bearings and gears.

A numeric approach has been developed to estimate the effect of Hertzian and non-Hertzian contact parameters in ball bearings, [3]. The analysis uses the slice technique for bearings with 2, 3 or 4 contact points. A computing code was developed in Borland Delphi and Visual Fortran to study these cases. The proposed equations retrieve the Hertz contact type and offer some realistic information about the cutting point contact.

ABAQUS/Standard was used to examine the Hertzian contact stress in two-dimension models before extending the study to three-dimension models, [4]. The general stress patterns in the needles are much closer to those in the 2-D model and the recorded contact pressures on the central needle are up to 80% of those recorded by the 2-D analysis. The comparative work using the 2-D and 3-D models as described was done in order to enable 3-D analysis involving bending in the bearing to be investigated.

A 3-D model of deep groove ball bearing was built by using APDL language embedded in the finite element software ANSYS. The obtained results have good consistency with that of the Hertzian theory, [5]. Through contact analysis, the changes could be showed in stress, strain, penetration, sliding distance, friction stress among the inner ring, outer ring, rolling elements and cage. Furthermore, the simulation results revealed that the computational values were consistent with theoretical values.The effect of the displacement of inner race and the friction coefficient on fatigue, wear, penetration and generated Hertzian stress was studied, [6]. It has been concluded that, an increase of the displacement of the inner race increases both of the Hertzian stress and the penetration.

The contact stress of large diameter ball bearings was studied using analytical and numerical methods, [7]. In analytical method, the contact stress is determined using the Hertzian Elliptical contact theory. The procedure of the calculation consists of a calculation for the maximum contact pressure on the rolling element using in-house developed program, and detailed finite element analysis of the contact between the ball and the raceway. Furthermore, the finite element analysis performed to predict contact pressure in ball and raceway where a comparison between the obtained results is carried.

The contact stress under different structural parameters are analyzed in detail and the changing laws of curvature coefficient, the number and diameter of the rolling element and contact stress are discussed, [8]. The 3D model is carried out for analyzing the effect of deep groove ball bearing structure parameters to the contact stress. The effect of the diameter and number of rolling element to contact stress is greater. With the increase in the diameter of the rolling element, the contact stress is gradually reduced. The same, the contact stress is also gradually reduced along with the increase in the number of rolling element, whose changing law close to linear relations.

A FEM and a semi analytical approach are used for load distribution calculation in statically radial loading, [9]. The finite element results are consistent and closer to analytical formulations in the case of rigid housing. A complex deformable housing is numerically integrated in a ball bearing to study the load distribution considering. The numerical results show that housing deformation has effect on load distribution.

The Lundberg-Palmgren theory considers the inverse of a 9th power relation between Hertz stress and fatigue life for ball bearings. The effect of race conformity on ball set life independent of race life is not incorporated into the Lundberg-Palmgren theory. It is concluded that, the actual bearing fatigue life is usually equal to or greater than that calculated using the ANSI/ABMA and ISO standards that incorporate the Lundberg-Palmgren theory, [10].Two simple algebraic relationships were established to calculate life factors to determine the effect of inner and outer race conformity combinations on bearing life for deep groove and angular contact ball bearings.

In the present study, two-dimension model for a sector of a ball bearing ball (Ball and a portion of the inner race) is created where the stress distribution of the bearing structure is performed using the finite element method. Also, a three-dimension model is proposed to simulate the effect of the force variation and shaft misalignment on the generated stresses. The contact stresses are calculated using the Hertzian theory of elastic deformation. The results of analytical and numerical solutions are compared.

ANALYSIS

Nomenclature

α	: Contact angle
υ_1, υ_2	: Poisson's ratio for the two spheres. apparent elastic modulus
σ_1 , σ_2 , σ_3	: Principle stresses
E_1 , E_2	: Young's modulus
a	: Radius of the contact area
F	: Acting force
P_{max}	: Maximum pressure
R_1 , R_2	: Radii of contact balls
Z	: depth of the contact area

1. Hertzian Contact Stress on Ball Bearing

The Hertzian theory of elastic deformation of contact between elastic bodies can be used to find contact areas and indentation depths for simple geometries. The theoretical contact area of two spheres is shown in Fig. 1.

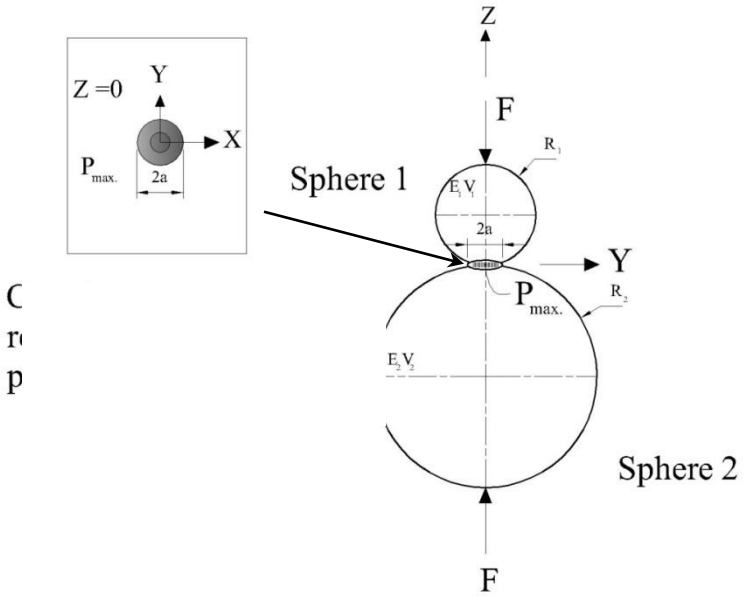

Fig. 1 Contact pressure between two spheres.

The radius of the contact area is given by:

$$a = \sqrt[3]{3F\left[\frac{1-\upsilon_1^2}{E_1}+\frac{1-\upsilon_2^2}{E_2}\right]\Big/4\left(\frac{1}{R_1}+\frac{1}{R_2}\right)} \quad (1)$$

The maximum contact pressure at the center of the circular contact area is:

$$P_{max} = 3F/2\pi a^2 \quad (2)$$

The principal stresses (σ_1,σ_2,σ_3) are:

$$\sigma_1 = \sigma_2 = -P_{max}[(1+\upsilon)\left\{1-\frac{z}{a}\tan^{-1}\frac{a}{z}\right\} - 1/2\,(\frac{z^2}{a^2}+1)] \quad (3)$$

$$\sigma_3 = -P_{max}(\frac{z^2}{a^2}+1)^{-1} \quad (4)$$

The analytical model is established using setting up a program in MATLAB. The model is equipped to calculate the value of contact pressure. The equations are fed to program with some assumption. Both of the ball and the race have the same material with elastic modulus "E" of 203 GPa and Poisson's ratio "υ" of 0.29. The bearing is simulated as a system which consists of a sphere – with radius R_1 of 3.175mm - in contact with a spherical groove. During the application of the Hertzian theory, the spherical groove has been considered as a sphere with a negative radius "R_2" of-3.5 mm. The load has the values of 1000, 2000, 3000, 4000 and 5000 N. Fig. 2 shows the flowchart of the MATLAB program.

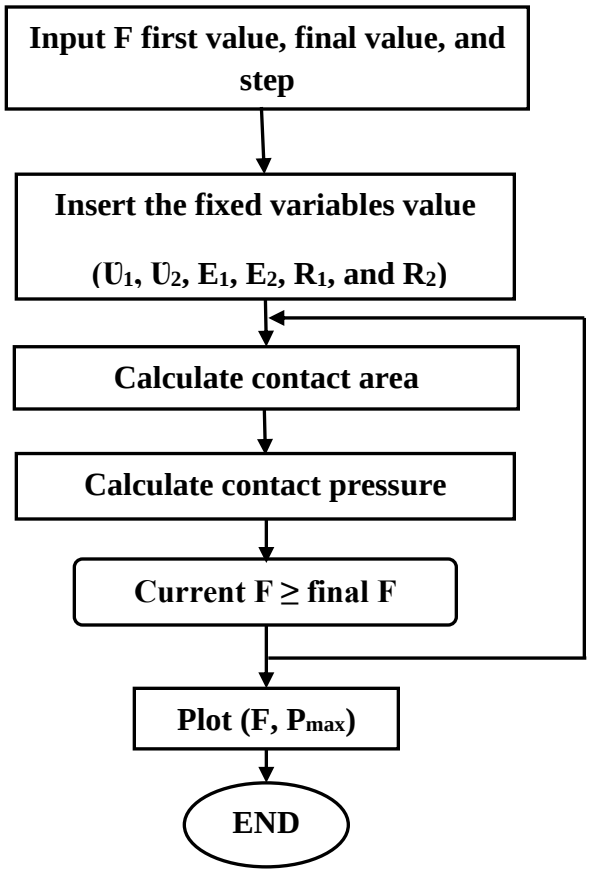

Fig. 2 MATLAB Flow chart.

2. Numerical Modeling

The bearing type; that has be used in this study; is a single row deep groove ball bearing with spare part number 6004 (SKF).

The bearing geometry is shown in Fig. 3. And its dimensions are:

- **Outer diameter, D_o = 42 mm,**
- **Bore diameter, D_i = 20 mm,**
- **Pitch diameter, d_m= 31 mm,**
- **Raceway width, B = 12 mm,**
- **Ball diameter, D = 6.35 mm,**
- **Contact angle, $\alpha = 0^0$,**
- **Raceway diameter of outer ring, d_0= 34.8 mm,**
- **Raceway diameter of inner ring, d_i= 27.2 mm.**

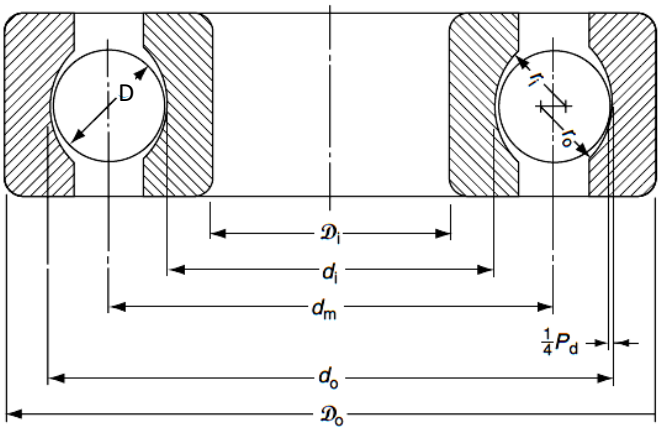

Fig. 3 Geometry of the deep groove ball bearing 6004.

2.1 Model Creation

2.1.1 Two-dimensional model

Finite element analysis offers many ways to analyze structures. It requires understanding of the program and the characteristics of the object. Element types included shell and solid elements can be used. The shell type can be take the form of linear or quadratic shape. These types has been considered and their results were compared. Here, two-dimensional models "Model I" and three dimensional models "Model II" has been studied. “Model I” is built as a ball and inner race. The creation of the model has been carried out through several steps. The first step is the drawing of the part using ABAQUS/CAE package where the part was considered as a planar deformable body with a shell base. The simulation has been carried out under the condition of isotropic material for both of ball and race with linear-elastic fracture mechanics. The material has a modulus of elasticity “E” of 203GPa and Poisson's ratio “v” of 0.29.The boundary conditions for two-dimensional model were chosen as illustrated in Fig. 4, where the race is fixed in all direction for displacement and rotation and the ball in the x- direction. The applied load (bearing redial load) acts the ball vertically in the negative y-direction.

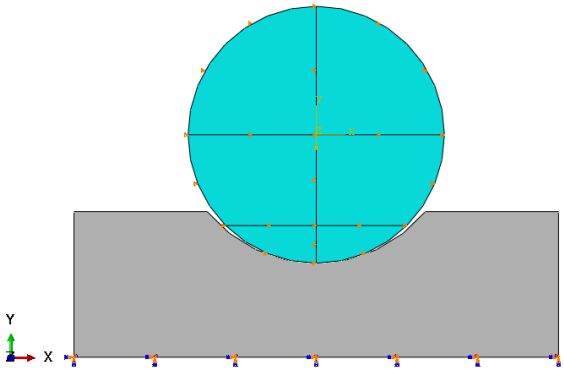

Fig. 4 The boundary condition of the two-dimensional Model.

The fulfillment of the creation of the two-dimensional model has been carried out using two-dimensional 4-node, fully integrated plane strain elements (CPE4R). The mesh was optimized by correlation to save running time. The structure technique mesh has been selected with higher degree of refinement, smaller element size and greater number of load cycles. Figure 5 shows the considered mesh.

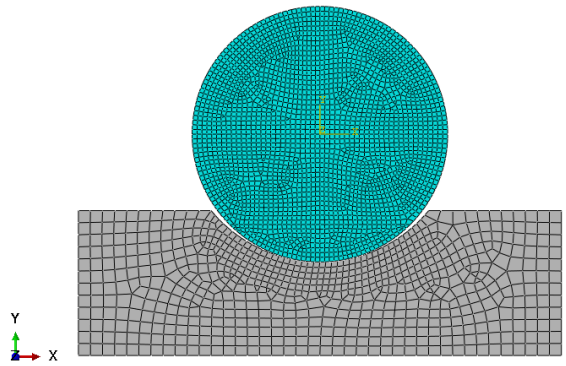

Fig. 5 The mesh of two-dimensional model.

3.1.2 Three-dimensional model

Model II is built as a three dimension sub model for the bearing and housing.It assumed also that, the bearing material is isotropic and linear-elastic fracture mechanics with modulus of elasticity "E" of 203GPa, Poisson's ratio "ν" of 0.29and density "ρ" of 7850 Kg/m^3. For the housing, the material is assumed to be isotropic and linear-elastic fracture mechanics with modulus of elasticity "E" of 195GPa, Poisson's ratio "ν" of 0.26and density "ρ" of 7300 Kg/m^3.In stead of coupling and rigid body constrains, the tie type has been used to join the outer race with the housing part.

The inner nodes of the inner race are coupled to the centered reference node, on which the radial load acts, Fig. 6. The formulation type of the common contact surface between the ball and races has been chosen to be penalty enforcement type with coefficient of friction of 0.1.

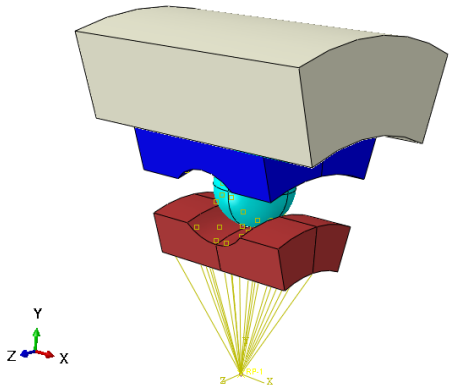

Fig. 6 Three-dimension Sub model of deep groove ball bearing.

The boundary conditions for the three-dimensional model are shown in Fig. 7. The housing part is fixed in three mutual perpendicular displacement directions (U1, U2, U3); mainly x-, y- and z-direction; as well as it is non-rotational about these axis(UR1, UR2, UR3). Furthermore, the ball is fixed in the two displacement directions (U1, U3) and as well as it is non rotational about the two axis UR2 and UR3. Moreover, the inner race can be rotate with an angular velocity about its axis and the race is stationary (i.e. V1=V3=0 & VR2 = VR3 = 0).For analyzing the contact in the 3-D models, a coarse mesh of solid elements with reduced integration and eight nodes (C3D8R) were used in the first instance. The reduced integration with eight nodes element (C3D8R) has been replaced with fully integrated, 8-node element (C3D8) to produce better quality for the contact surface stresses. Figure 8 shows the mesh with the fully integrated, 8-node elements (C3D8).

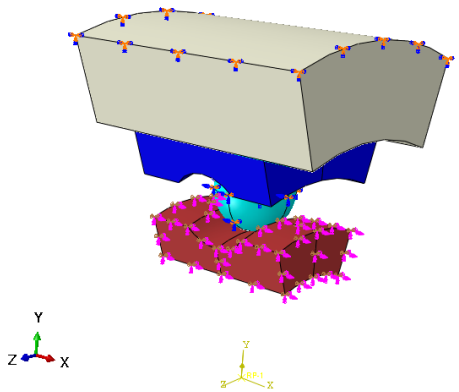

Fig. 7 The boundary condition of Model II.

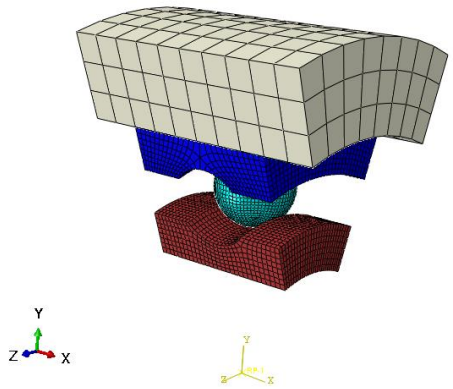

Fig. 8 The mesh of the three-dimensional model with C3D8-elements.

RESULTS AND DISCUSSIONS

The generated contact stress has been determined at certain variable using the Hertzian contact theory. Based on the Hertzian contact theory, the contact stress for variable load condition is calculated using MATLAB a program and compared with the same stresses that have been obtained from the finite element model. Figure 9 illustrate the relation between the contact stress and the applied load which has been obtained from Hertzian theory.

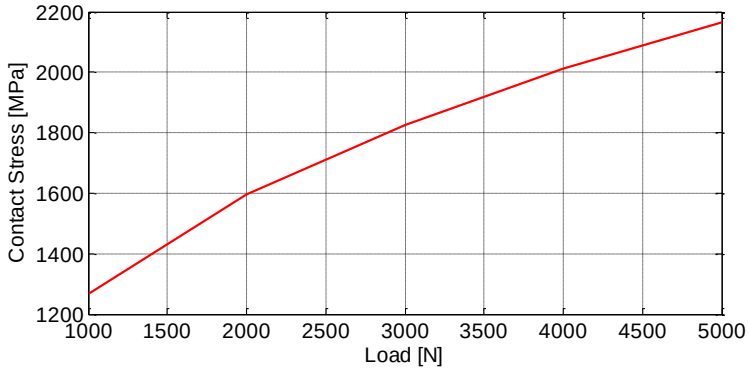

Fig. 9 Contact stress versus the applied load according to Hertzian theory.

Comparison between the results of the Hertzian theory and that of the two- and three-dimensional models shows that a good agreement between the results. The stress distribution of the contact stress; that has been obtained from the simulation; on the inner race is shown in Fig. 10. It can be noticed that, the maximum stress is located in the center of the inner surface of the race, i.e. at the point of action of the external applied load.

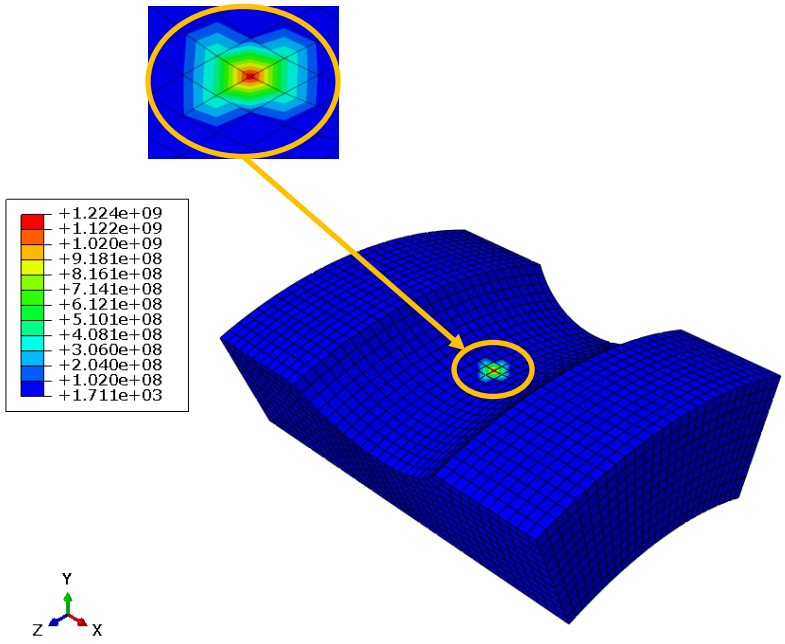

Fig. 10 Maximum stress distribution at the acting point on the inner race.

Figure10 shows the stress distribution on the contact of the inner race from the three-dimension model. The maximum stress is located in the center of the inner surface of the race at the point of action of the applied force. The results of both analytical and FEA treatments are compared and plotted in Fig. 11. The figure shows that, the results are nearly similar with a variation of about 3.5%.

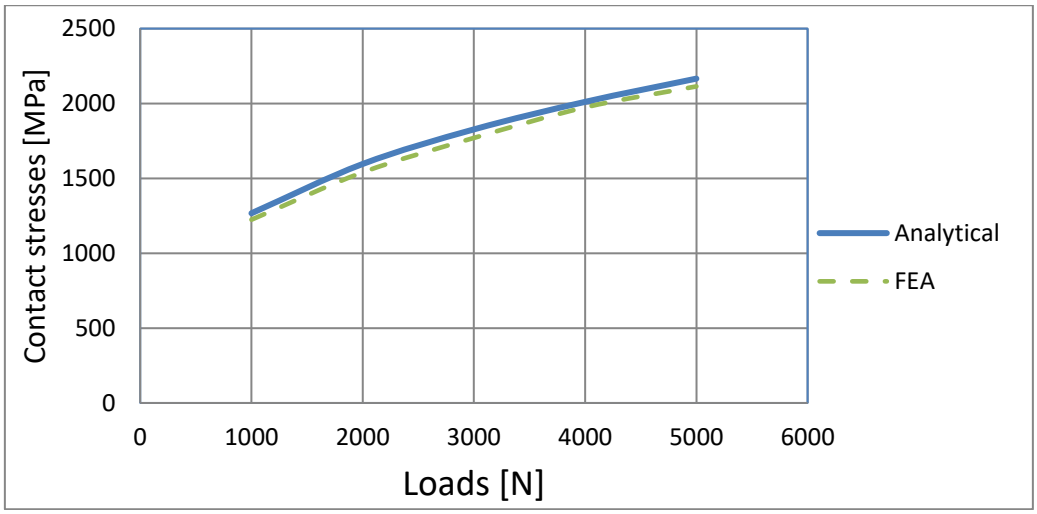

Fig. 11 Comparison between the Hertzian and numerically contact stresses.

The stress distribution along the thickness of the race material can be determined using the two-dimensional modeling as shown in Fig.12. Furthermore, two-dimensional model

has a greater distinct in comparison to the three-dimensional model where a great computational time cost can be saved.

Figure 13 shows the stress distribution versus the contact width. It is noticed that, the contact pressure concentration at the central zone of the contact area is nearly similar to that of the Hertz formulas. However, the analytical model cannot be used to calculate the stress distribution due to the effect of the loads at the longitudinal path of the contact area.

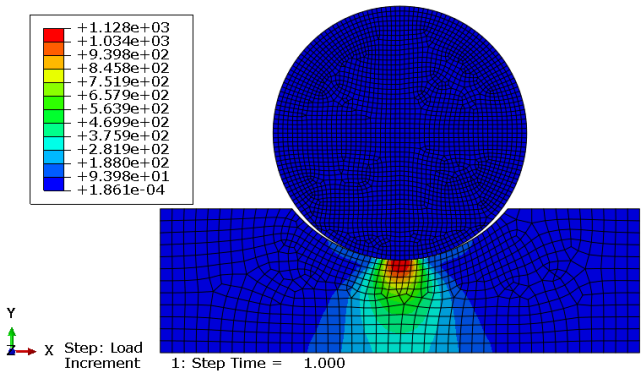

Fig. 12 Stress distribution across the race thickness according to the two-dimensional model.

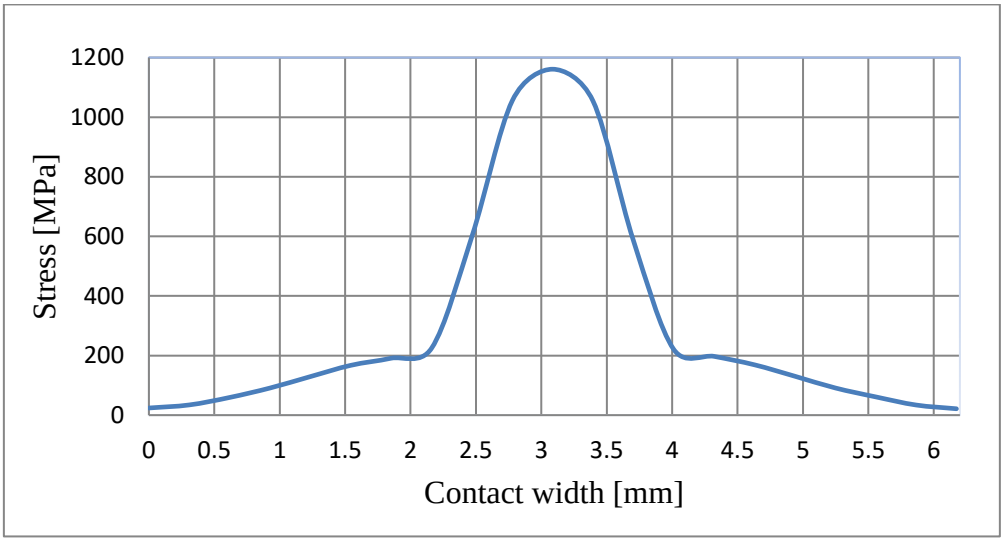

Fig. 13 Stress Distribution versus contact width.

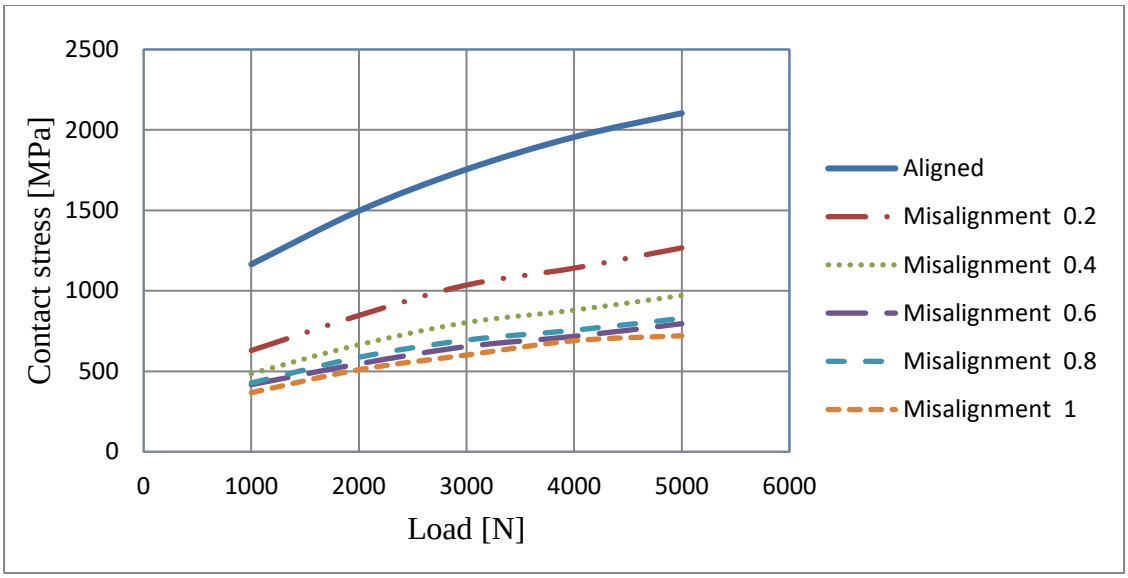

Fig. 14 Contact stress versus acting load for different shaft misalignment angles.

The effect of the shaft misalignment has been investigated by the help of the two- and three-dimensional modeling, where the inner race has been displaced with angles of 0.2^0, 0.4^0, 0.6^0, 0.8^0 and 1^0. Figure 14 shows the variation of the maximum stress versus the load at different misalignment angles. It can be noticed that, the generated stress decreases with the increase of the misalignment angle. This phenomenon can be related to the increase of the contact area between the ball and the inner race at the point of action of load. Therefore, Fig. 15 illustrates the relationship between the generated contact stress and the width of the contact zone, where a decrease of the maximum stress has been noticed by the increase of the contact width. . Furthermore, the position of the peak of the maximum stress is shifted with a certain value by the increase of the contact width. Nevertheless, it can be predicted that, the probability of wear occurrence increases with the increase of the frictional area.

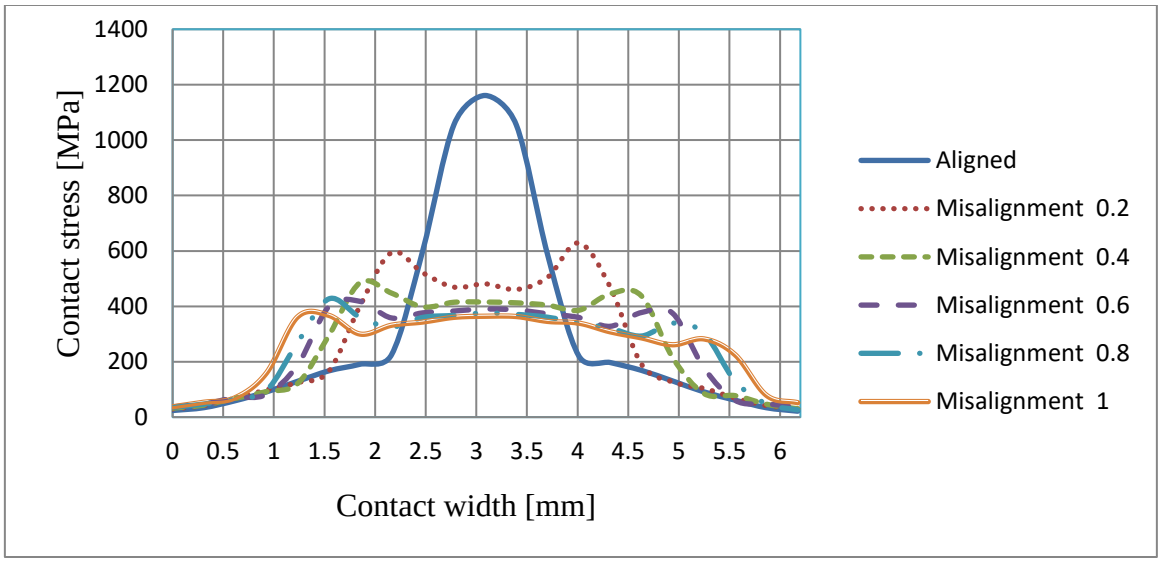

Fig. 15Contact stress versus contact widthat different shaft misalignment angles.

CONCLUSIONS

Based on the results from the Hertzian contact theory and the numerical treatment using ABAQUS/CAE, the following conclusions can be drawn:

1. **The finite element analysis can predict contact stress in ball and raceway.**
2. **The stress distribution along the inner race thickness can be achieved from the two-dimensional simulation.**
3. **The results of two- and three- dimensional modeling are quite similar where the two-dimensional model has the advantage of computational time saving.**
4. **The maximum stress decreases with the increase of the contact width.**
5. **The peak of the maximum stress is positioned in the middle of the contact width for alignment shaft and it will be shifted with a certain value as the contact width increases due to shaft misalignment.**

REFERENCES

1. Harris T. A., Kotzalas M. N., "Essential Concepts of Bearing Technology", Taylor & Francis Group, (2006).

2. Hertz H., "On Contact of Solid Elastic Bodies and on Hardness", Journal of Mathematics, Vol. 92, pp. 156–171, (1881).

3. Rezmires D., Nelias D., Racocea C., "Hertzian and Non-Hertzian Contact Analysis in Ball Bearings", The Annals of University "DUNĂREA DE JOS "of Galaţi Fascicle VIII, (2004).

4. Furbatto L., King S., "Investigation into the distribution of contact pressure in roller bearings used for high speed automotive applications", ABAQUS Users' Conference, (2007).

5. Tang Z., Sun J., "The Contact Analysis for Deep Groove Ball Bearing Based on ANSYS", Procedia Engineering, Vol. 23, pp. 423 – 428, (2011).
6. Dahiya S. K., Jain A. K., "Analysis of Deep Groove Ball Bearing Using ANSYS", VSRD International Journal, Vol. 3 No. 1, (2013).
7. Pandiyarajan R., Starvin M. S., Ganesh K. C., "Contact Stress Distribution of Large Diameter Ball Bearing Using Hertzian Elliptical Contact Theory", Procedia Engineering, Vol. 38, pp. 264 - 269, (2012).
8. Yujuan X., Geni M., Lu R. B., "Optimization of Deep Groove Ball Bearing Contact Interface Parameters and Strength Evaluation", the International Conference on Fracture & Strength of Solids, (2013).
9. Ayao E. A., Debray K., Bolaers F., Chiozzi P., Palleschi F., "Modeling of the Behavior of a Deep Groove Ball Bearing in Its Housing", Journal of Applied Mathematics and Physics, VOL. 1, pp. 45 - 50, (2013).
10. Zaretsky E., Poplawski J., Root L., "Relation between Hertz Stress-Life Exponent, Ball-Race Conformity, and Ball Bearing Life", Tribology Transaction, VOL. 51, 2; pp. 150–159, (2008).